The mineralocorticoid receptor (MR) regulates ENaC but not NCC in mice with random MR deletion

Czogalla, Jan ; Vohra, Twinkle ; Penton, David ; Kirschmann, Moritz ; Craigie, Eilidh ; Loffing, Johannes

Abstract: Aldosterone binds to the mineralocorticoid receptor (MR) and increases renal Na+ reabsorption via up-regulation of the epithelial Na+ channel (ENaC) and the Na+-K+- ATPase in the collecting system (CS) and possibly also via the NaCl cotransporter (NCC) in the distal convoluted tubule (DCT). However, whether aldosterone directly regulates NCC via MR, or indirectly through systemic alterations remains controversial. We used mice with deletion of MR in 20% of renal tubule cells (MR/X mice), in which MR-positive (MRwt) and -negative (MRko) cells can be studied sideby- side in the same physiological context. Adult MR/X mice showed similar mRNA and protein levels of renal ion transport proteins to control mice. In MR/X mice, no differences in NCC abundance and phosphorylation was seen between MRwt and MRko cells and dietary Na+ restriction up-regulated NCC to similar extent in both groups of cells. In contrast, MRko cells in the CS did not show any detectable alpha- ENaC abundance or apical targeting of ENaC neither on control diet nor in response to dietary Na+ restriction. Furthermore, Na+-K+-ATPase expression was unaffected in MRko cells of the DCT, while it was lost in MRko cells of the CS. In conclusion, MR is crucial for ENaC and Na+-K+-ATPase regulation in the CS, but is dispensable for NCC and Na+-K+-ATPase regulation in the DCT.

DOI: https://doi.org/10.1007/s00424-016-1798-5

The mineralocorticoid receptor (MR) regulates ENaC but not NCC in mice with random MR deletion

Jan Czogalla[1,3], Twinkle Vohra[1], David Penton[1,3], Moritz Kirschmann[2], Eilidh Craigie[1,3], Johannes Loffing[1,3]

[1]Institute of Anatomy, University of Zurich, Zurich, Switzerland;

[2]Center for Microscopy and Image Analysis, University of Zurich, Zurich, Switzerland;

[3]Swiss National Centre for Competence in Research "Kidney control of homeostasis"

Running head

NCC regulation is MR independent

Corresponding author

Johannes Loffing

Institute of Anatomy, University of Zurich

Winterthurerstrasse 190, CH-8057 Zurich

Switzerland

Phone: +41 (0) 44 635 53 20

Fax: + 41 (0) 44 635 57 02

Email: johannes.loffing@anatom.uzh.ch

ACKNOWLEDGEMENTS

The authors would like to thank Günter Schütz and Stefan Berger, Burkhard Becher, Celso E. Gomez-Sanchez, and Eric Feraille for kindly providing us with the MRlox/lox mouse line, the cmv-cre mouse line, the anti-MR antibodies, and the anti-Na^+-K^+-ATPase antibody, respectively. The expert technical assistance by Monique Carrel and Michèle Heidemeyer is gratefully acknowledged.

GRANTS

This work was supported the Swiss National Center for Competence in Research "Kidney.CH" and by a project grant (310030_143929/1) from the Swiss National Science Foundation. David Penton is a postdoctoral fellow of the Marie-Curie program within the European Union's 7^{th} framework program for research, technological development and demonstration under the grant agreement no. 608847.

DISCLOSURES The authors declare no conflict of interest, financial or otherwise.

ABSTRACT

Aldosterone binds to the mineralocorticoid receptor (MR) and increases renal Na^+ reabsorption via up-regulation of the epithelial Na^+ channel (ENaC) and the Na^+-K^+-ATPase in the collecting system (CS) and possibly also via the NaCl cotransporter (NCC) in the distal convoluted tubule (DCT). However, whether aldosterone directly regulates NCC via MR, or indirectly through systemic alterations remains controversial. We used mice with deletion of MR in ~20% of renal tubule cells (MR/X mice), in which MR-positive (MR^{wt}) and -negative (MR^{ko}) cells can be studied side-by-side in the same physiological context. Adult MR/X mice showed similar mRNA and protein levels of renal ion transport proteins to control mice. In MR/X mice, no differences in NCC abundance and phosphorylation was seen between MR^{wt} and MR^{ko} cells and dietary Na^+ restriction up-regulated NCC to similar extent in both groups of cells. In contrast, MR^{ko} cells in the CS did not show any detectable alpha-ENaC abundance or apical targeting of ENaC neither on control diet nor in response to dietary Na^+ restriction. Furthermore, Na^+-K^+-ATPase expression was unaffected in MR^{ko} cells of the DCT, while it was lost in MR^{ko} cells of the CS. In conclusion, MR is crucial for ENaC and Na^+-K^+-ATPase regulation in the CS, but is dispensable for NCC and Na^+-K^+-ATPase regulation in the DCT.

Keywords: distal tubule, mineralocorticoid receptor, ncc, aldosterone

INTRODUCTION

Aldosterone (aldo) is important for the control of sodium (Na^+) homeostasis and hence extracellular volume and blood pressure. It stimulates Na^+ reabsorption in aldo-sensitive epithelia in the kidney, colon, and sweat glands and elicits its effects by binding to the mineralocorticoid receptor (MR). The MR acts as a transcription factor controlling expression and activity of proteins either mediating or regulating epithelial Na^+ transport [2, 21, 32]. The importance of the MR for Na^+ homeostasis is underlined by the observation that in humans loss-of-function mutations in the MR cause renal salt wasting and hyperkalemia despite high plasma aldosterone levels (pseudohypoaldosteronism) [8]. Likewise, mice with targeted inactivation of the MR die shortly after birth due to severe extracellular volume depletion if not rescued by repeated subcutaneous NaCl injections [3, 4].

In the kidney, aldosterone stimulates Na^+ reabsorption by activating the epithelial Na^+ channel (ENaC) and the basolateral Na^+-K^+-ATPase in the segment-specific epithelial cells of the renal connecting tubule (CNT) and collecting duct (CD), which together form the collecting system (CS) [22]. Renal MR expression is not restricted to the CS, but is also found in the distal convoluted tubule (DCT) and the thick ascending limb (TAL) [2, 5]. Increased plasma levels of aldosterone induced by exogenous aldosterone infusion, dietary Na^+ restriction or diuretic treatment correlate with an increased abundance and phosphorylation of the thiazide-sensitive NaCl cotransporter (NCC) in the DCT [11, 12, 34, 35]. The stimulatory effect of aldosterone on NCC was also reported to occur in DCT cells in vitro and was suggested to involve the activation of various different kinases including SGK1 [32], WNK4 [34], and SPAK [12] as well as the ubiquitin ligase Nedd4-2 [14, 27]. Pharmacological blockade of the MR by spironolactone inhibited, at least part, the effects of

aldosterone on the DCT and NCC [16], suggesting that the MR mediated the effects of aldosterone on NCC. Nevertheless, it remains unclear whether the effects of aldosterone on NCC are mediated directly via the MR or might be secondary to changes provoked at the systemic levels. For example, hyperaldosteronism causes hypokalemia [20] which is known to profoundly affect NCC [25, 29]. Moreover, it is important to note that the enzyme 11-β-hydroxysteroid-dehydrogenase type 2 (11βHSD2), protecting the MR from activation by glucocorticoids through rapid metabolization of cortisol in humans and corticosterone in rodents, is significantly expressed only in the endportion of the DCT (DCT2) and the CS [2, 5, 10]. Therefore, this expression pattern of 11βHSD2 raises the important question of how aldosterone can activate the MR in the DCT in the presence of 100-1000 times higher glucocorticoid plasma levels.

To address the role of the MR in NCC regulation, we took advantage of the fact that in cells of female animals one of the two X chromosomes is permanently and randomly inactivated. Thus, mating of mice with a X-chromosome-linked expression of the cre recombinase [24] with mice with floxed MR alleles [21] generated female mice carrying a targeted deletion of MR in some, but not all, of their cells (MR/X mice). In this model, MR-positive (MR^{wt}) and MR-negative (MR^{ko}) cells can be studied next to each other in the same physiological context. This model is highly advantageous as it provides an excellent internal control for any differential effects of confounding factors provoked at the systemic level (e.g. compensatory upregulation of hormones and/or altered tubular flow and extracellular ion concentration).

MATERIAL AND METHODS

Animals. All animal experiments were conducted according to Swiss Laws and approved by the veterinary administration of the Kanton of Zürich, Switzerland. MR/X mice were generated on a C57Bl/6 background by breeding homozygous $MR^{lox/lox}$ males with homozygous $MR^{lox/lox}$ females in addition heterozygous for the X-chromosome linked cmv-cre [24]. All experiments were done in female mice homozygous for $MR^{lox/lox}$ and heterozygous for cmv-cre expression (MR/X). Female $MR^{lox/lox}$/cmv-cre wt mice were used as control.

Rescue protocol: In our first breeding program, MR^{ko} mice did not survive. To improve survival of newborn MR^{ko} mice, the rescue protocol suggested by Bleich et. al. for MR ko mice was applied [4]. After weaning, animals were given standard chow and water *ad libitum*.

Metabolic cages: Mice were studied for 4 days in metabolic cages, receiving 2 days of control (0.3% NaCl)- and 2 days of 0.03% NaCl diet (Sniff Spezialdiäten, Soest, Germany). At the end of the experiment, either blood and kidneys were harvested and snap-frozen or kidneys were fixed by vascular perfusion with 3% paraformaldehyde/0.1 M phosphate buffer as previously described [25]**.**

Aldosterone and corticosterone measurements. Plasma was diluted 1:5, urine was diluted 1:50 and both were measured in triplicates using an aldosterone ELISA Kit (CAN-ALD-450, Diagnostics Biochem Canada Inc., Canada) or a corticosterone ELISA Kit (Cayman Chemical, Ann Arbor, Michigan) and a Tecan plate reader (Tecan infinite F200 pro, Tecan Group AG, Switzerland) according to manufacturer's instructions.

Electrolyte analysis. Urine electrolyte levels were measured in 100 µl urine diluted 1:10 in dH_2O using an EFOX 5053 flame photometer (Eppendorf, Eppendorf,

Germany). Plasma electrolyte composition was analyzed with a radiometer ABL 80 flex (Radiometer Medical ApS, Brønshøj, Denmark) immediately after venous blood sampling.

Realtime PCR. Total kidney RNA was isolated using a Nucleospin RNA kit (Macherey Nagel). The real-time PCR was performed using a LightCycler 480 Instrument II (Roche, Basel, Switzerland). The following primers have been used: MR forward: TTCGGAGAAAGAACTGTCCTG; MR reverse: CCCAGCTTCTTTGACTTTCG; GR forward: CAAAGATTGCAGGTATCCTATGAA; GR reverse: TGGCTCTTCAGACCTTCCTT; 11 ß-HSD2 forward: CCAGCAGGAGACATGCCATAC; 11 ß-HSD2 reverse: GCTGACCTTGATACCCCAGG; αENaC, forward: ACCCCGTGAGTCTCAACATC; αENaC reverse: CCTGGCGAGTGTAGGAAGAG; γENaC forward: AGTTCAGAAAGAACTCTGCAGGC; γENaC reverse: GTGTTCAGGCAGTACCAATGC; NCC forward: TGACCTGCATTCATTCCTCA; NCC reverse: GAAGCGAACAGGTTCTCCAG; ß-actin forward: CCACCGATCCACACAGAGTACTT; ß-actin reverse: GACAGGATGCAGAAGGAGATTACTG.

Immunoblotting. Whole kidneys were homogenized by ultrasound in lysis buffer as previously described [25]. Protein concentration was assessed via Bradford assay (CooAssay Protein Dosage Reagent, Uptima, France). 25µg of protein were solubilized in loading buffer (31.5 mmol/L Tris-HCl, 1% SDS, 0.005% Bromphenolblue, 12.5% glycerol and 5% ß-mercaptoethanol, pH 6.5), run in SDS PAGE and transferred to nitrocellulose membranes. Secondary dye-conjugated antibody fluorescence (IRDye, Li-Cor Biosciences, USA) was imaged using a Li-Cor

infrared scanner (Li-Cor Biosciences, USA). Optical density was quantified using ImageJ software (***http://imagej.nih.gov/ij/***).

Immunofluorescence. Kidneys were processed for immunofluorescence as described previously [25]. For MR staining, microwave heating was used for antigen retrieval followed by the Tyramide Signal Amplification protocol as proposed by the manufacturer (TSA Fluorescein System, Perkin Elmer, Waltham, MA USA). Microwave heating reduced the nuclear DAPI staining and caused a general cytoplasmic background that appears in the composite immunofluorescence images as grey staining. Images were acquired using a Leica TCS SP8 upright confocal microscope and processed by ImageJ software. Composite immunofluorescence images are presented in magenta/green/grey to increase contrast for the deuteranomalic population.

Morphometry. For quantification of MR knockdown, two whole kidney sections each of four MR^{ko} animals were scanned at 10x. Six fields of view (FOV) were evenly scattered at random locations over the kidney cortex and placed the same for every image. DCT and CS were determined via morphological criteria. Cells in the FOV were visually assigned to be either MR^{wt} or MR^{ko}.

Immunofluorescence intensity quantification. Optical density of IF stainings was determined using ImageJ software (http://imagej.nih.gov/ij/) with a custom script to minimize bias. Sections from eight MR^{ko} animals, four having received for two days 0.03 % Na^+ diet and four having received control diet, were scanned with a Leica TCS SP8 upright confocal microscope at 20x magnification with a numerical aperture of 0.99. At least four orthogonally cut DCTs and CSs each per animal were randomly selected for quantification. The investigator defined the center of the tubule from which then a circle with the radius of 35 µm was automatically generated and

subdivided into 360 equal sectors. Subsequently, the centers of MR-labeled or unlabeled cells were selected based on the fluorescence signal of MR. For each cell and each channel, the staining intensity of ten sectors was integrated. Within a 10° angle, the intensity of the staining at the apical or basolateral cell side was quantified. The script is available in the supplement.

Reagents and antibodies. Unless otherwise stated, reagents were purchased from Sigma Aldrich (Sigma, Buchs, Switzerland). Antibodies directed against total and phosphorylated NCC (tNCC and pT53NCC), αENaC and γENaC were previously described [17, 25, 37]. The anti-MR antibody was kindly provided by Dr. Gomez-Sanchez [9]. The anti-Na^+-K^+-ATPase antibody was a kind gift from Dr. Feraille [7]. Antibodies have been used in the following dilutions for immunoblotting: anti-GR: 1:2.000; anti-11-ß-HSD-2: 1:1.000; anti-αENaC: 1:5.000; anti- γENaC: 1:10.000; anti-tNCC: 1:5.000; anti-pT53NCC: 1:5.000; anti-ß-actin: 1:20.000. Antibody dilutions for immunofluorescence were: anti-MR: 1:40; anti-αENaC: 1:10.000; anti-γENaC: 1:20.000; anti-tNCC: 1:40.000; anti-pT53NCC: 1:200.000; anti-Na^+-K^+-ATPase: 1:20.000; Nuclei were stained with DAPI: 1:500.

Statistical Analysis. Results are expressed as means ± SEM. ANOVA Kruskal-Wallis test with Holm-Sidak's multiple comparisons test was applied unless otherwise specified.

RESULTS

Similar to whole-body MR knockout mice [4], MR/X mice died within ~10 days after birth, unless they were rescued by Na^+ supplementation according to the protocol by Bleich and co-workers (Fig. 1a, b). However, in contrast to whole-body knockout mice, MR/X mice thrive normally and do not exhibit any significant growth retardation once the critical postnatal phase is overcome. RT-PCR (Fig. 2a) and immunoblots (Fig. 2b) did not show any difference in the expression of GR, 11-ß-HSD2, alpha and gamma subunits of ENaC, and NCC between kidney homogenates of adult control and MR/X mice. MR expression as studied by immunofluorescence revealed no obvious differences between both groups of mice in overviews of the kidney (Fig. 2c). However, detailed analysis revealed that the MR was lost in the MR/X mice in 27.44 ± 3.50 % (*n* = 4) and 16.63 ± 2.16 % (*n* = 4) of the DCT and CS cells, respectively. As the inactivation of the X chromosome occurs randomly, MR inactivation was expected in ~50 % of the cells. The unexpected low number of cells with MR deletion could possibly be explained by an inefficient cre-expression or by a selection advantage of MR^{wt} over MR^{ko} cells.

We next challenged control and MR/X mice with two days of dietary Na^+ restriction (0.03% Na^+) to try to reveal possible compensation defects. Urinary Na^+ excretion dropped significantly, while 24 h urinary aldosterone and K^+ excretion increased compared to control diet in both groups of mice. The 24 h urine volumes increased slightly, but were not significantly different from the values measured under control diet in both groups of mice (Fig. 3). Likewise, plasma electrolytes did not show any significant differences between genotypes (Table 1). Interestingly, the dietary sodium restriction lowered plasma K^+ concentration in both groups of mice (Table 1).

Independent from the underlying mechanism for the unexpected low number of cells with MR deletion, the MR/X mice permitted us to study MR^{wt} and MR^{ko} cells side-by-side in the same kidney. To quantify immunofluorescent staining intensities for individual cells, we developed an ImageJ script (Supplement) that automatically analyzes optical densities of fluorescence in given areas around the axis of orthogonally sectioned tubules. With this approach, we were able to accurately measure fluorescence intensities in single cells in the same tubular profile in an unbiased way (Fig. 4). First, we analyzed by immunofluorescence NCC expression and phosphorylation using antibodies against total NCC and NCC phosphorylated at serine 53. We found that the subcellular localization and the abundance of total and phosphorylated NCC was similar in MR^{wt} and MR^{ko} during control conditions (Fig. 5). In response to feeding a low Na^+ diet, total NCC and phospho-NCC staining increased to similar extents in both MR^{wt} and MR^{ko} cells (Fig. 5a). Thus, the presence or absence of MR expression does not determine the level of NCC abundance and phosphorylation under control conditions and does not control the up-regulation of NCC in response to dietary Na^+ restriction.

We next analyzed αENaC and γENaC expression in the CS. Under control conditions, αENaC staining intensity was significantly lower in MR^{ko} than in MR^{wt} cells, while γENaC staining intensity was significantly enhanced in knockout cells (Fig. 6a). However, γENaC was not targeted to the apical plasma membrane and was found diffusely distributed throughout the cytoplasm in MR^{ko} cells (Fig. 6c). Two days of dietary Na^+ restriction further increased αENaC staining intensity in MR^{wt} cells (Fig. 6a), while αENaC remained almost undetectable in MR^{ko} cells. Consistent with an impaired aldosterone-dependent regulation of ENaC, the MR^{ko} cells also did not show any translocation of γENaC to the apical cell surface as was evident in the MR^{wt} cells (Fig. 6b, c).

The rate of Na^+ reabsorption along the renal tubule does not only depend on the activity of the apical Na^+ transporting proteins, but also on the Na^+-K^+-ATPase in the basolateral plasma membrane. In the CS, the expression and the activity of the Na^+-K^+-ATPase is regulated via aldosterone and the MR [30]. In the DCT, the role of aldosterone and the MR for the Na^+-K^+-ATPase is less clear [19, 26]. Therefore, we next investigated the expression of the Na^+-K^+-ATPase in MR^{wt} and MR^{ko} cells. In DCTs, loss of MR did not cause any change to the abundance of the Na^+-K^+-ATPase, under neither control- nor under low sodium diet conditions (Fig. 7). However, in the CS, the loss of the MR significantly lowered Na^+-K^+-ATPase expression (Fig. 7).

DISCUSSION

The aldosterone - MR signaling axis is critical for ion- and extracellular volume homeostasis, as highlighted in our study by the 100% perinatal lethality of the MR/X mice. It therefore seems that during the very critical perinatal phase [15, 23] a loss of the MR in less than half of the cells of the body is sufficient to provoke a life-threatening situation if the renal Na^+ loss is not replaced by parenteral Na^+ supplementation.

Given that there is no X-chromosomal-linked MR-deficiency in humans, our chosen experimental approach is artificial. However, the employed transgenic mouse model enabled us to study the cell autonomous role of the MR in intact animals. By comparing MR^{wt} and MR^{ko} cells in the same tubule of the same kidney in the same mouse, we achieved a perfect internal control for any confounding factor provoked at the systemic level. Together with the developed automated quantification system, we could efficiently quantify immunofluorescent signals for the MR, total and phosphorylated NCC, ENaC, and the Na^+-K^+-ATPase in individual tubular epithelial cells. The detected significant differences for MR and ENaC immunostainings between MR^{wt} and MR^{ko} cells support the reliability of our approach. The detected significant up-regulation of total and phospho-NCC abundance in DCT cells of mice on a low Na^+ diet reproduced previous immunoblotting results [11] and demonstrated that the chosen approach can be used to compare immunostaining intensities between different groups of mice.

Although we were able to detect a stimulation of NCC by dietary Na^+ restriction, we did not find any evidence for a regulatory role of the MR for NCC abundance and phosphorylation. This contrasts with the conclusions drawn from several previous in vivo studies in which the effect of Na^+ restriction [11, 35], aldosterone infusion [11,

35], furosemide-treatment [1], and MR inhibition [16] on NCC was studied at the level of the whole animal. However, all these experimental maneuvers do not only change plasma aldosterone levels and/or interfere with MR signaling, but may provoke numerous confounding effects on plasma hormone levels and/or tubular flow that may interfere with NCC regulation as well. For example, Na^+ restriction, diuretic treatment and MR inhibition activate the renin-angiotensin system, and angiotensin II is a known potent NCC regulator [13, 33]. Likewise, aldosterone- as well as furosemide administration cause hypokalemia, which may activate NCC by direct effects on DCT plasma membrane voltage, intracellular chloride concentrations, and WNK/SPAK activity [29]. Interestingly, we also observed that the two days of dietary sodium restriction lowered plasma K^+ levels in mice. Consistent with a dominant role of plasma K^+, two groups were just able to show that the down-regulation of NCC in mice with kidney-specific MR deletion could be overcome or at least mitigated by employing dietary K^+ restriction to normalize plasma K^+ [6, 28]. Likewise, recent studies using mice deficient for 11βHSD2 by Hunter and colleagues challenged the conventional concept of mineralocorticoid signaling in the DCT [10]. The possible contribution of non-genomic effects of aldosterone on NCC regulation is intriguing and awaits future studies [18].

In contrast to NCC, the MR appears to be critical for the regulation of ENaC. Under control conditions, the MR^{ko} cells in the CS did not show any detectable αENaC expression or apical localization of ENaC. Dietary Na^+ restriction failed to up-regulate αENaC and to translocate the channel to the cell surface in MR^{ko} cells, which is consistent with the results of many previous studies including those analyzing mouse models with a constitutive or an inducible inactivation of the MR in the CNT and CD [2, 21, 31]. Interestingly, although the loss of the MR did not interfere with the abundance of the Na^+-K^+-ATPase in the DCT, it did in the CS of the MR/X mice. The

loss of the Na^+-K^+-ATPase in the MR^{ko} cells of the CS might be a direct consequence of the impaired transcriptional regulation of the pump or the indirect result of the lowered apical Na^+ entry rate due to the down-regulation of ENaC [30, 36, 38]. Independent from the underlying mechanism our data suggest that the expression of both the apical and basolateral Na^+ transport pathways in the CS are dependent on the presence of the MR, while the MR expression is dispensable in the DCT.

In conclusion, we describe an easy-to-use, microscopy-based, semi-quantitiative approach to study the cell autonomous role of a regulatory protein of renal Na^+ transport in the context of an intact animal. Our data confirm the crucial relevance of the MR for ENaC and Na^+-K^+-ATPase regulation in the CS, but challenge the current concepts on the importance of the aldosterone-MR signaling axis for the control of NCC and ion transport regulation in the DCT. Our chosen approach might also prove useful to test the relevance of other signaling molecules that are proposed to regulate both ENaC and NCC, for instance Sgk1, Nedd4-2 and the WNKs.

FIGURE LEGENDS

Fig. 1 Successful rescue of MR/X mice. **(a**) Survival of newborn MR/X mice receiving 25µl/g bw 0.9% NaCl s.c. from day 2 pp (**dashed line,** *n* = 7) compared to wildtype animals receiving same injections (**continuous line,** *n* = 9) and MR/X mice receiving no injections (**dotted line,** *n* = 7). (**b**) MR/X mice receiving NaCl gained bodyweight comparable to wt, while no more significant bodyweight gain after day 5 pp was notable in the mutant group receiving no injections

Fig. 2 Adult MR/X mice are unchanged from control mice at the whole kidney level. (**a**) Whole kidney mRNA expression in MR/X mice is not significantly different to control (ctr) mice in realtime-PCR. Data expressed as change in percent to values of ctr mice ± SEM. While MR and GR message did show a tendency to be alleviated in MR/X mice, this trend did not reach significance. *n* = 4 for ctr & MR/X. (**b**) Whole kidney protein expression for the glucocorticoid receptor (GR), the 11-beta-hydroxysteroid dehydrogenase type 2 (11-β-HSD 2), the full length and the proteolytically cleaved (arrows) forms of alpha and gamma subunits of the epithelial sodium channel (ENaC), and of total (t) and phosphorylated (pT53) NCC is similar for control (Ctr) and MR/X mice. Densitometric measurements did not reveal any significant differences between groups (not shown). Detection of ß-actin served as loading control. (**c**) Overview of MR staining in MR/X mice does not reveal gross differences to wildtype control. Inset: representative image of a MR/X DCT compared to a control DCT. MR loss shows a clustered pattern of 1-5 cells next to each other throughout the whole kidney

Fig. 3 Urinary volumes and urinary aldosterone, Na^+ and K^+ excretion are almost similar for control (Ctr) and MR/X mice under standard diet and in response to 2 days of a low Na^+ diet. Data are expressed as means ± SEM, $n \geq 4$ for ctr, $n \geq 7$ for MR/X

Fig. 4 Scheme of the ImageJ script for quantification of optical density of MR staining in orthogonally cut DCTs. A user defines the center of the distal tubule based only on the fluorescence signal of the apical target protein (Step 1). Based on this input a circle with the radius of 35 µm is generated which automatically subdivides into 360 equal sectors (Step 2). Subsequently, the centers of MR-labeled or unlabeled cells are user-selected based on the fluorescence signal of MR (Step 3, "x" for positive, "y" for negative). For each cell and each channel, the staining intensity of ten sectors in its direction is automatically integrated (Step 4). Via this, staining of 10° of membrane apical from the nucleus is quantified

Fig. 5 Neither total NCC (tNCC) abundance nor NCC phosphorylation (pT53 NCC) are affected by loss of MR. (**a**) NCC expression and phosphorylation increase significantly in response to low Na^+ diet in cells with and cells without MR to the same extent. $n \geq 19$ cells for all conditions, * $P < 0.05$ in Kruskal-Wallis test with Holm-Sidak's multiple comparisons test. Representative immunofluorescent images for total NCC (**b**) and pT53 NCC (**c**) under both control (upper panels) and low Na^+ diet (lower panels). Control animals shown for comparison. DAPI background staining shown in composite images in grey. Arrows point to cells with MR deletion. *Scale bars:* 10 µm

Fig. 6 ENaC is affected by MR loss. (**a**) In MR^{ko} cells of mice on a control diet, αENaC staining intensity is significantly lower, while γENaC staining intensity is significantly higher than in MR^{wt} cells. Under low Na^+ diet, αENaC staining intensity increases in MR^{wt} cells, while it remains very low in MR^{ko} cells. γENaC staining intensity remains unchanged in both groups of mice. $n \geq 19$ cells for all conditions, * $P < 0.05$ in Kruskal-Wallis test with Holm-Sidak's multiple comparisons test. Representative immunofluorescent images for αENaC (**b**) and γENaC (**c**). Control

animals shown for comparison. DAPI background staining shown in composite images in grey. Arrows point to cells with MR deletion. Asterisks mark intercalated cells. *Scale bar:* 10 µm

Fig. 7 Na^+-K^+-ATPase is not affected by loss of MR in DCTs, but is affected by loss of MR in the collecting system (CS). (**a**) In DCTs, Na^+-K^+-ATPase staining intensity is unchanged in response to loss of MR under both control and low Na^+ diet. In the collecting system, Na^+-K^+-ATPase staining is lost in MR^{ko} cells, independent of the dietary condition. $n \geq 19$ cells for all conditions, * $P < 0.05$ in Kruskal-Wallis test with Holm-Sidak's multiple comparisons test. (**b**) Representative immunofluorescent images for DCT (left panel) and CS (right panel) under both control (upper panels) and low Na^+ diet (lower panels). Control animals shown for comparison. DAPI background staining shown in grey. Arrows point to cells with MR deletion. Asterisks mark intercalated cells. *Scale bar:* 10 µm

REFERENCES

1. Abdallah JG, Schrier RW, Edelstein C, Jennings SD, Wyse B, Ellison DH (2001) Loop diuretic infusion increases thiazide-sensitive Na(+)/Cl(-)-cotransporter abundance: role of aldosterone. J Am Soc Nephrol 12:1335–1341.

2. Ackermann D, Gresko N, Carrel M, Loffing-Cueni D, Habermehl D, Gomez-Sanchez C, Rossier BC, Loffing J (2010) In vivo nuclear translocation of mineralocorticoid and glucocorticoid receptors in rat kidney: differential effect of corticosteroids along the distal tubule. Am J Physiol Renal Physiol 299:F1473–F1485.

3. Berger S, Bleich M, Schmid W, Greger R, Schutz G (2000) Mineralocorticoid receptor knockout mice: Lessons on Na+ metabolism. Kidney Int 57:1295–1298.

4. Bleich M, Warth R, Schmidt-Hieber M, Schulz-Baldes A, Hasselblatt P, Fisch D, Berger S, Kunzelmann K, Kriz W, Schütz G, Greger R (1999) Rescue of the mineralocorticoid receptor knock-out mouse. Pflugers Arch 438:245–254.

5. Bostanjoglo M, Reeves WB, Reilly RF, Velázquez H, Robertson N, Litwack G, Morsing P, Dørup J, Bachmann S, Ellison DH (1998) 11Beta-hydroxysteroid dehydrogenase, mineralocorticoid receptor, and thiazide-sensitive Na-Cl cotransporter expression by distal tubules. J Am Soc Nephrol 9:1347–1358.

6. Canonica J, Sergi C, Maillard M, Klusonova P, Odermatt A, Koesters R, Loffing-Cueni D, Loffing J, Rossier B, Frateschi S, Hummler E (2016) Adult nephron-specific MR-deficient mice develop a severe renal PHA-1 phenotype. Pflugers Arch 1–14.

7. Carranza ML, Féraille E, Favre H (1996) Protein kinase C-dependent phosphorylation of Na(+)-K(+)-ATPase alpha-subunit in rat kidney cortical tubules. Am J Physiol Cell Physiol 271:C136–C143.

8. Geller DS, Rodriguez-Soriano J, Vallo Boado A, Schifter S, Bayer M, Chang SS, Lifton RP (1998) Mutations in the mineralocorticoid receptor gene cause autosomal dominant pseudohypoaldosteronism type I. Nat Genet 19:279–281.

9. Gomez-Sanchez CE, de Rodriguez AF, Romero DG, Estess J, Warden MP, Gomez-Sanchez MT, Gomez-Sanchez EP (2006) Development of a Panel of Monoclonal Antibodies against the Mineralocorticoid Receptor. Endocrinology 147:1343–1348.

10. Hunter RW, Ivy JR, Flatman PW, Kenyon CJ, Craigie E, Mullins LJ, Bailey MA, Mullins JJ (2014) Hypertrophy in the Distal Convoluted Tubule of an 11β-Hydroxysteroid Dehydrogenase Type 2 Knockout Model. J Am Soc Nephrol 26:1537–1548.

11. Kim GH, Masilamani S, Turner R, Mitchell C, Wade JB, Knepper MA (1998)

The thiazide-sensitive Na-Cl cotransporter is an aldosterone-induced protein. Proc Natl Acad Sci USA 95:14552–14557.

12. Ko B, Mistry AC, Hanson L, Mallick R, Wynne BM, Thai TL, Bailey JL, Klein JD, Hoover RS (2013) Aldosterone acutely stimulates NCC activity via a SPAK-mediated pathway. Am J Physiol Renal Physiol 305:F645–F652.

13. Lee DH, Maunsbach AB, Riquier-Brison AD, Nguyen MTX, Fenton RA, Bachmann S, Yu AS, McDonough AA (2013) Effects of ACE inhibition and ANG II stimulation on renal Na-Cl cotransporter distribution, phosphorylation, and membrane complex properties. Am J Physiol Cell Physiol 304:C147–C163.

14. Loffing-Cueni D, Flores SY, Sauter D (2006) Dietary sodium intake regulates the ubiquitin-protein ligase nedd4-2 in the renal collecting system. J Am Soc Nephrol 17:1264–1274.

15. Martinerie L, Viengchareun S, Delezoide A-L, Jaubert F, Sinico M, Prevot S, Boileau P, Meduri G, Lombès M (2009) Low Renal Mineralocorticoid Receptor Expression at Birth Contributes to Partial Aldosterone Resistance in Neonates. Endocrinology 150:4414–4424.

16. Nielsen J, Kwon T-H, Masilamani S, Beutler K, Hager H, Nielsen S, Knepper MA (2002) Sodium transporter abundance profiling in kidney: effect of spironolactone. Am J Physiol Renal Physiol 283:F923–33.

17. Picard N, Trompf K, Yang C-L, Miller RL, Carrel M, Loffing-Cueni D, Fenton RA, Ellison DH, Loffing J (2014) Protein phosphatase 1 inhibitor-1 deficiency reduces phosphorylation of renal NaCl cotransporter and causes arterial hypotension. J Am Soc Nephrol 25:511–522.

18. Quinn SA, Harvey BJ, Thomas W (2014) Rapid aldosterone actions on epithelial sodium channel trafficking and cell proliferation. Steroids 81:43–48.

19. Reilly RF, Ellison DH (2000) Mammalian distal tubule: physiology, pathophysiology, and molecular anatomy. Physiol Rev 80:277–313.

20. Rojas-Vega L, Gamba G (2016) Mini-review: regulation of the renal NaCl cotransporter by hormones. Am J Physiol Renal Physiol 310:F10–4.

21. Ronzaud C, Loffing J, Bleich M, Gretz N, Gröne H-J, Schütz G, Berger S (2007) Impairment of sodium balance in mice deficient in renal principal cell mineralocorticoid receptor. J Am Soc Nephrol 18:1679–1687.

22. Rossier BC, Staub O, Hummler E (2013) Genetic dissection of sodium and potassium transport along the aldosterone-sensitive distal nephron: Importance in the control of blood pressure and hypertension. FEBS Letters 587:1929–1941.

23. Schmidt K, Ripper M, Tegtmeier I, Humberg E, Sterner C, Reichold M, Warth R, Bandulik S (2013) Dynamics of Renal Electrolyte Excretion in Growing Mice. Nephron Physiol 124:7–13.

24. Schwenk F, Baron U, Rajewsky K (1995) A cre-transgenic mouse strain for the ubiquitous deletion of loxP-flanked gene segments including deletion in germ cells. Nucleic Acids Res 23:5080–5081.

25. Sorensen MV, Grossmann S, Roesinger M, Gresko N, Todkar AP, Barmettler G, Ziegler U, Odermatt A, Loffing-Cueni D, Loffing J (2013) Rapid dephosphorylation of the renal sodium chloride cotransporter in response to oral potassium intake in mice. Kidney Int 83:811–824.

26. Stanton BA, Kaissling B (1989) Regulation of renal ion transport and cell growth by sodium. Am J Physiol 257:F1–10.

27. Staub O, Abriel H, Plant P, Ishikawa T, Kanelis V (2000) Regulation of the epithelial Na+ channel by Nedd4 and ubiquitination. Kidney Int 57:809–815.

28. Terker AS, Yarbrough B, Ferdaus MZ, Lazelle RA, Erspamer KJ, Meermeier NP, Park HJ, McCormick JA, Yang CL, Ellison DH (2015) Direct and Indirect Mineralocorticoid Effects Determine Distal Salt Transport. J Am Soc Nephrol 1–10.

29. Terker AS, Zhang C, McCormick JA, Lazelle RA, Zhang C, Meermeier NP, Siler DA, Park HJ, Fu Y, Cohen DM, Weinstein AM, Wang W-H, Yang C-L, Ellison DH (2015) Potassium Modulates Electrolyte Balance and Blood Pressure through Effects on Distal Cell Voltage and Chloride. Cell Metabolism 21:39–50.

30. Therien AG, Blostein R (2000) Mechanisms of sodium pump regulation. Am J Physiol Cell Physiol 279:C541–66.

31. Todkar A, Picard N, Loffing-Cueni D, Sorensen MV, Mihailova M, Nesterov V, Makhanova N, Korbmacher C, Wagner CA, Loffing J (2015) Mechanisms of renal control of potassium homeostasis in complete aldosterone deficiency. J Am Soc Nephrol 26:425–438.

32. Vallon V, Huang DY, Grahammer F, Wyatt AW, Osswald H, Wulff P, Kuhl D, Lang F (2005) SGK1 as a determinant of kidney function and salt intake in response to mineralocorticoid excess. Am J Physiol Regul Integr Comp Physiol 289:R395–R401.

33. van der Lubbe N, Lim CH, Fenton RA, Meima ME, Danser AHJ, Zietse R, Hoorn EJ (2010) Angiotensin II induces phosphorylation of the thiazide-sensitive sodium chloride cotransporter independent of aldosterone. Kidney Int 79:66–76.

34. van der Lubbe N, Lim CH, Meima ME, van Veghel R, Rosenbaek LL, Mutig K, Danser AHJ, Fenton RA, Zietse R, Hoorn EJ (2012) Aldosterone does not require angiotensin II to activate NCC through a WNK4–SPAK–dependent pathway. Pflugers Arch 463:853–863.

35. Velázquez H, Bartiss A, Bernstein P, Ellison DH (1996) Adrenal steroids stimulate thiazide-sensitive NaCl transport by rat renal distal tubules. Am J Physiol 270:F211–9.

36. Vinciguerra M, Deschênes G, Hasler U, Mordasini D, Rousselot M, Doucet A, Vandewalle A, Martin P-Y, Féraille E (2003) Intracellular Na+ controls cell surface expression of Na,K-ATPase via a cAMP-independent PKA pathway in mammalian kidney collecting duct cells. Mol Biol Cell 14:2677–2688.

37. Wagner CA, Loffing-Cueni D, Yan Q, Schulz N, Fakitsas P, Carrel M, Wang T, Verrey F, Geibel JP, Giebisch G, Hebert SC, Loffing J (2008) Mouse model of type II Bartter's syndrome. II. Altered expression of renal sodium- and water-transporting proteins. Am J Physiol Renal Physiol 294:F1373–F1380.

38. Wang YB, Leroy V, Maunsbach AB, Doucet A, Hasler U, Dizin E, Ernandez T, de Seigneux S, Martin PY, Féraille E (2014) Sodium Transport Is Modulated by p38 Kinase-Dependent Cross-Talk between ENaC and Na,K-ATPase in Collecting Duct Principal Cells. J Am Soc Nephrol 25:250–259.

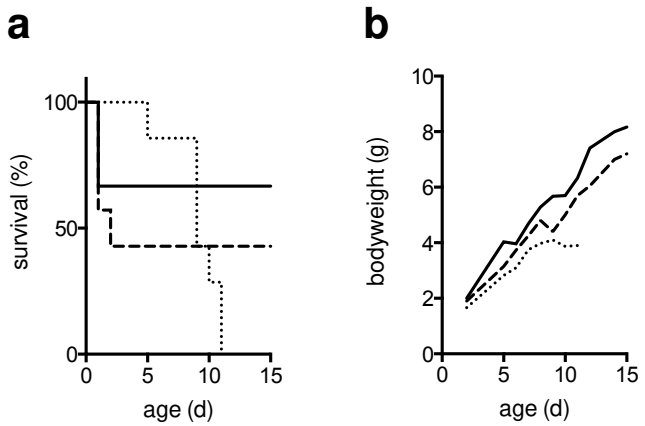

Figure 1
Czogalla et al, 2015

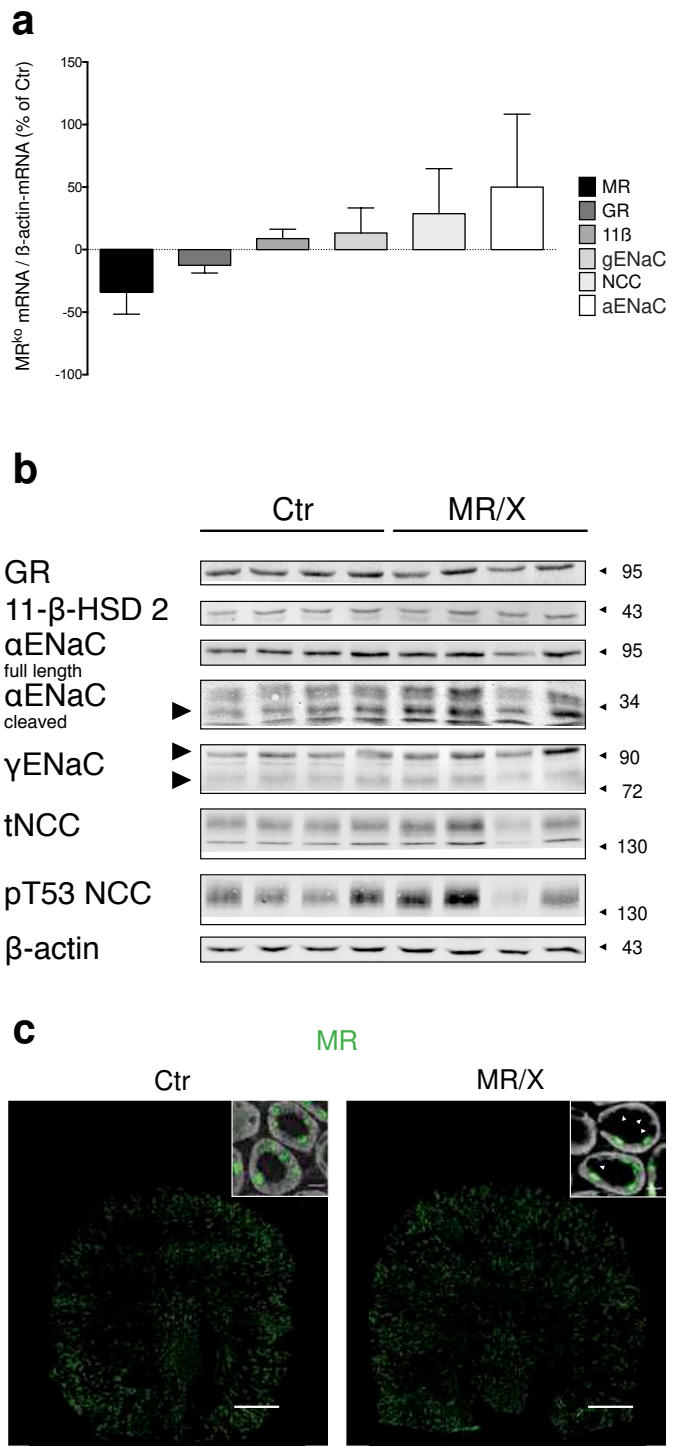

Figure 2
Czogalla et al, 2015

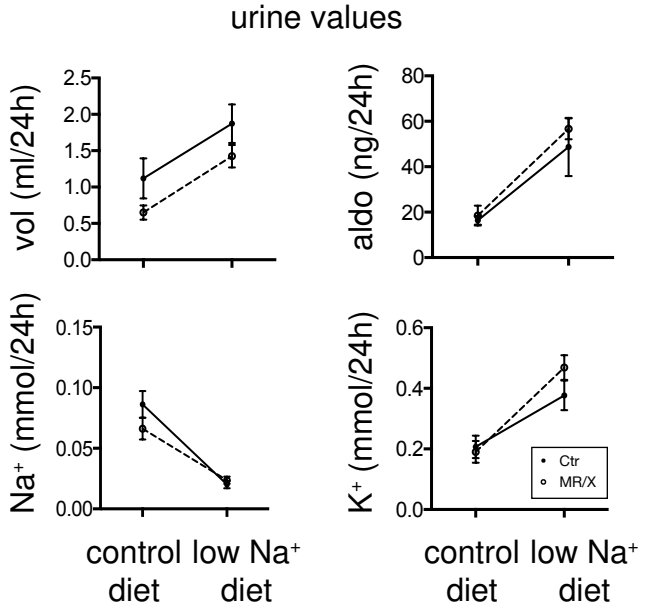

Figure 3
Czogalla et al, 2015

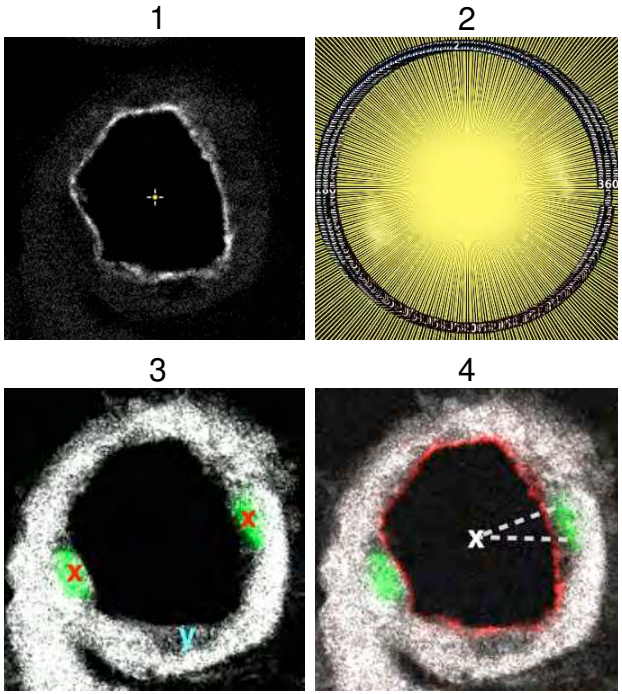

Figure 4
Czogalla et al, 2015

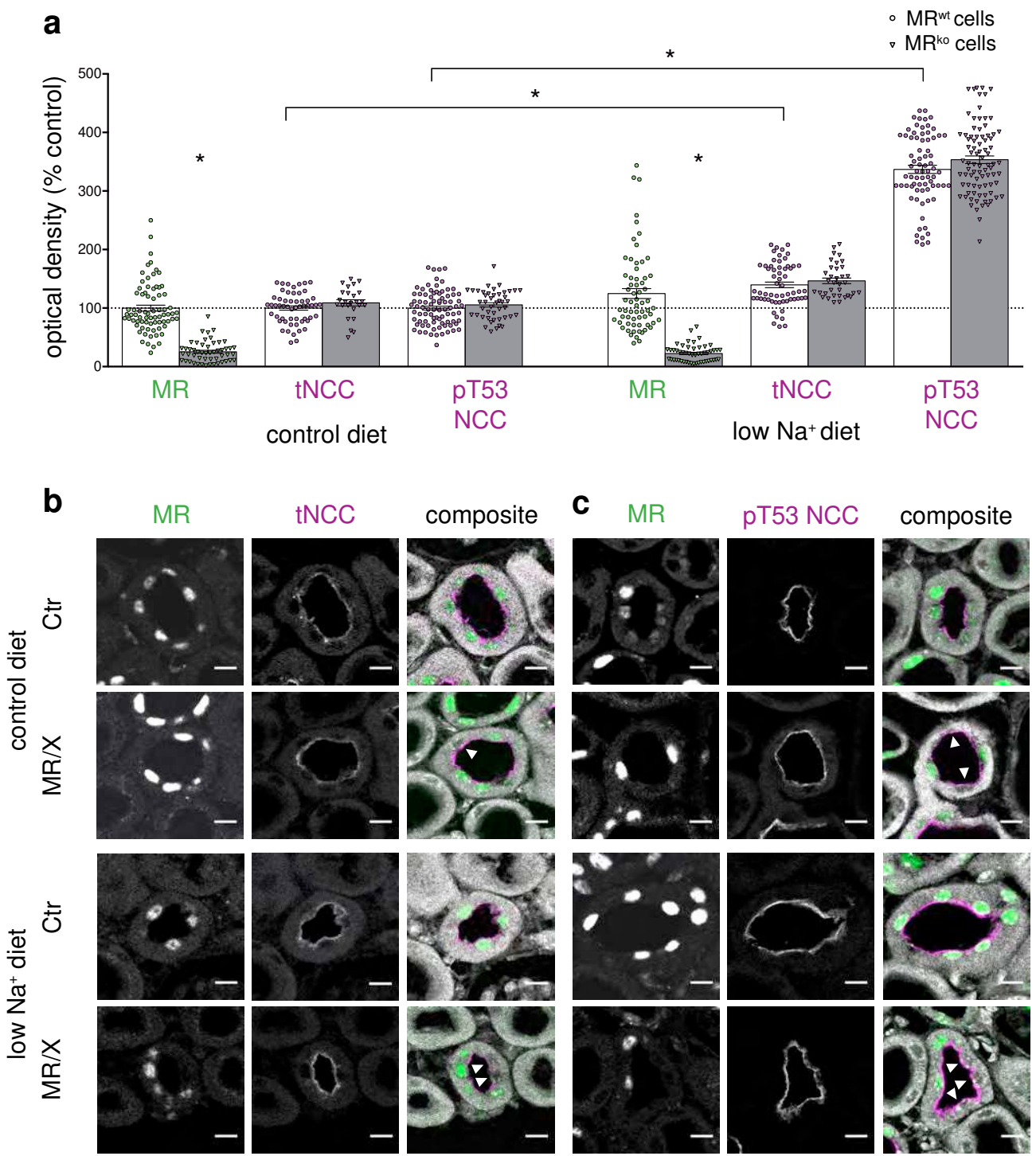

Figure 5
Czogalla et al,
2015

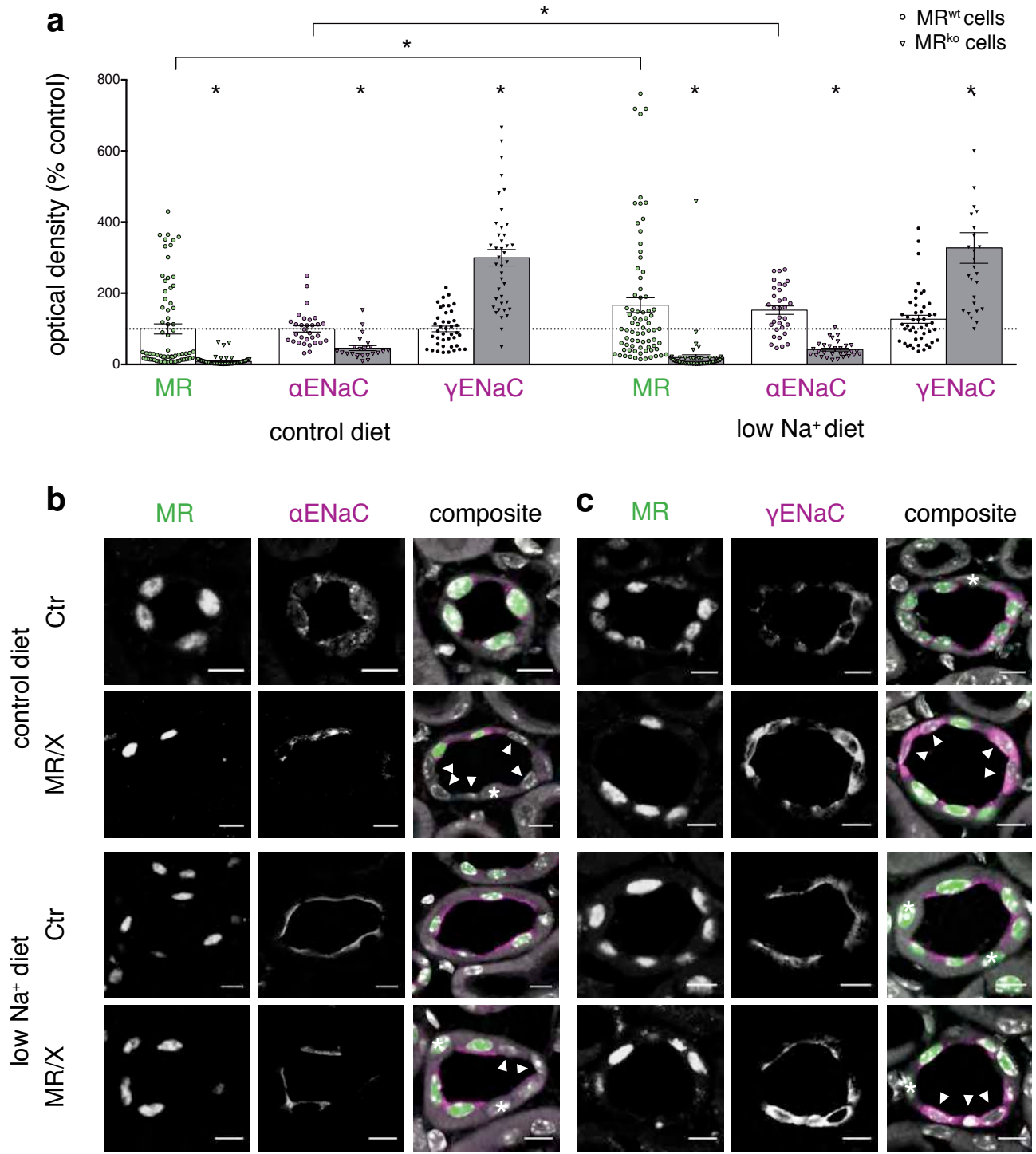

Figure 6
Czogalla et al, 2015

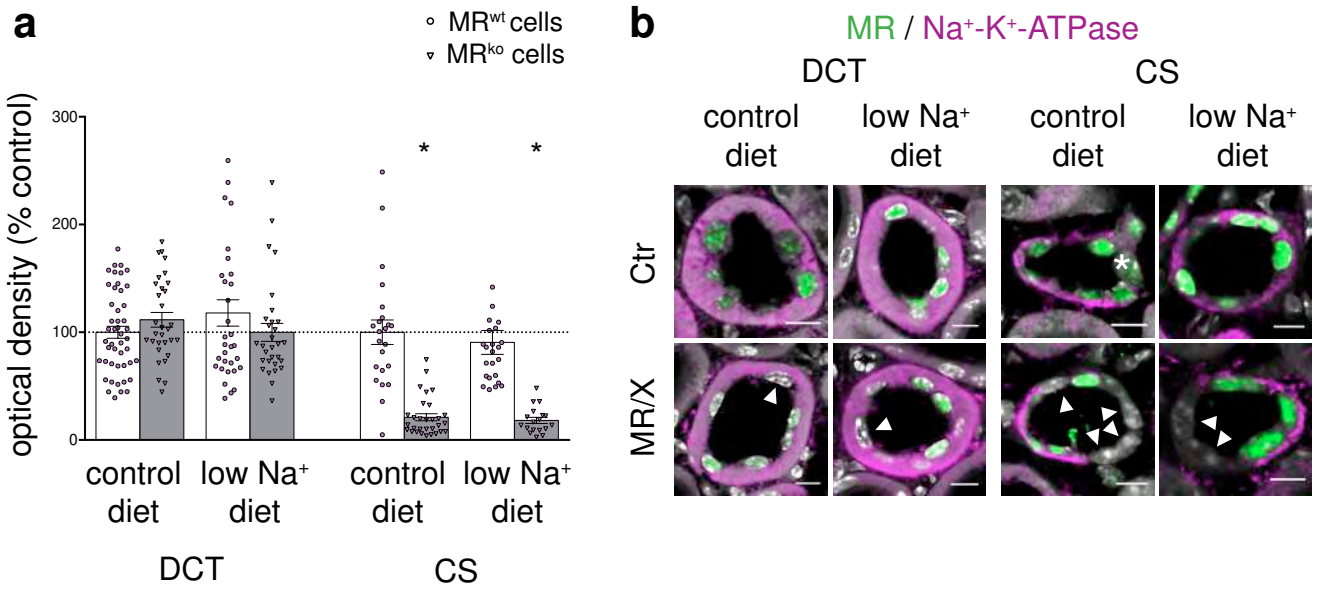

Figure 7
Czogalla et al, 2015

Table:

The mineralocorticoid receptor (MR) regulates ENaC but not NCC in mice with random MR deletion

Jan Czogalla[1,3], Twinkle Vohra[1], David Penton[1,3], Moritz Kirschmann[2], Eilidh Craigie[1,3], Johannes Loffing[1,3]

[1]Institute of Anatomy, University of Zurich, Zurich, Switzerland;

[2]Center for Microscopy and Image Analysis, University of Zurich, Zurich, Switzerland;

[3]Swiss National Centre for Competence in Research "Kidney control of homeostasis"

Corresponding author

Johannes Loffing

Institute of Anatomy, University of Zurich

Winterthurerstrasse 190, CH-8057 Zurich

Switzerland

Phone: +41 (0) 44 635 53 20

Fax: + 41 (0) 44 635 57 02

Email: johannes.loffing@anatom.uzh.ch

Table 1

Plasma parameters of control and MR/X mice on control- and after 2 days of a low Na^+ diet

Parameter	control	MR/X
	control diet	
n	5	5
pH	7.3 (±0.0)	7.3 (±0.0)
Na^+ (mmol/l)	144.4 (±0.6)	146.5 (±1.1)
K^+ (mmol/l)	5.1 (±0.4)	5.6 (±0.1)
Cl^- (mmol/l)	105.9 (±0.8)	108.3 (±1.6)
Ca^{2+} (mmol/l)	1.0 (±0.1)	1.1 (±0.1)
	low Na^+ diet	
n	6	4
pH	7.3 (±0.0)	7.2 (±0.0)
Na^+ (mmol/l)	146.0 (±0.0)	148.3 (±0.9)
K^+ (mmol/l)	3.1 (±0.1)	3.1 (±0.3)
Cl^- (mmol/l)	109.6 (±0.9)	105.7 (±1.3)
Ca^{2+} (mmol/l)	1.1 (±0.0)	1.0 (±0.1)

Values are expressed as means ± SE, *n* number of mice